Open Access **Baghdad Science Journal** **P-ISSN: 2078-8665**
Published Online First: April, 2023 **2023, 20(6): 2322-2329** **E-ISSN: 2411-7986**

DOI: https://dx.doi.org/10.21123/bsj.2023.7076

Numerical Investigation of Physical Parameters in Cardiac Vessels as a New Medical Support Science for Complex Blood Flow Characteristics

***Defrianto*[1]** ***Toto Saktioto*[1*]** ***Yan Soerbakti*[1]**
***Andika Thoibah*[1]** ***Bunga Meyzia*[1]** ***Romi Fadli Syahputra*[2]** ***Okfalisa*[3]**
***Syamsudhuha*[4]** ***Dedi Irawan*[5]** ***Haryana Hairi*[6]**

[1]Department of Physics, Faculty of Mathematics and Natural Sciences, Universitas Riau, Pekanbaru, Indonesia.
[2]Department of Physics, Faculty of Mathematics and Natural Sciences and Health, Universitas Muhammadiyah Riau, Pekanbaru, Indonesia.
[3]Department of Informatics Engineering, Faculty of Sciences and Technology, Universitas Islam Negeri Sultan Syarif Kasim, Pekanbaru, Indonesia.
[4]Department of Mathematics, Faculty of Mathematics and Natural Sciences, Universitas Riau, Pekanbaru, Indonesia.
[5]Department of Physics Education, Faculty of Teacher Training and Education, Universitas Riau, Pekanbaru, Indonesia.
[6]Department of Physics, Faculty of Applied Sciences, Universiti Teknologi MARA, Shah Alam, Malaysia.
*Corresponding author: saktioto@lecturer.unri.ac.id
E-mail addresses: defrianto@lecturer.unri.ac.id, yansoerbakti2@gmail.com, andika.thoibah@student.unri.ac.id, bungameyzia@gmail.com, romifadlisyahputra@yahoo.com, okfalisa@gmail.com, syamsudhuha@lecturer.unri.ac.id, dedi.irawan@lecturer.unri.ac.id, haryana.hairi@johor.uitm.edu.my

Received 20/2/2022, Revised 21/2/2023, Accepted 23/2/2023, Published Online First 20/4/2023, Published 01/12/2023

Abstract:

This study proposes a mathematical approach and numerical experiment for a simple solution of cardiac blood flow to the heart's blood vessels. A mathematical model of human blood flow through arterial branches was studied and calculated using the Navier-Stokes partial differential equation with finite element analysis (FEA) approach. Furthermore, FEA is applied to the steady flow of two-dimensional viscous liquids through different geometries. The validity of the computational method is determined by comparing numerical experiments with the results of the analysis of different functions. Numerical analysis showed that the highest blood flow velocity of 1.22 cm/s occurred in the center of the vessel which tends to be laminar and is influenced by a low viscosity factor of 0.0015 Pa.s. In addition, circulation throughout the blood vessels occurs due to high pressure in the heart and the pressure becomes lower when it returns from the blood vessels at the same parameters. Finally, when the viscosity is high, the extreme magnitudes of blood flow tend toward the vessel wall at approximately the same velocity and radius of the gradient.

Keywords: Blood flow, Finite element analysis,Heart, Navier-Stokes,Vessels.

Introduction:

Cardiovascular modelling continues to evolve due to the different kinematic movements of blood flow[1]. The heart has many movements involving complex interactions between viscous incompressible fluids and objects that can be deformed[2,3]. Meanwhile, the complex development of the cardiovascular system has led to the development of several designs and models to solve the problem of blood flow using several parameters[4]. These include the Reynolds number problem, the uncompressed Navier-Stoke equation in modelling blood dynamics, momentum equation on the blood flow of the heart.

The blood flow simulation system is very complicated, due to the difference in pressure at the time of entry and exit from the heart[5]. Furthermore, the complication occurs because of the three-dimensional concept of circulation using boundary conditions of where the blood exits and the diversity of the viscosity coefficient in the human body[6]. The use of hemodynamic simulation is one of the solutions to cardiovascular flow complications since the method is commonly used in scientific and

clinical studies as a statistical approach[7]. Furthermore, it is used in the correlation between near-wall blood flow parameters including shear wall pressure with existing cardiovascular disease[8–10]. Therefore, the use of hemodynamics is crucial for further study.

The study of the literature on circulatory disorders has been widely discussed[5,11]. However, several studies have shown that the porous walls of arteries can be deformed and at the same time the non-Newtonian nature of blood flow is different in the geometry of the vessels. To solve the problems in the interaction of the blood-fluid structure, a nonlinear approach and an incompressible viscosity flow field, or other approaches partition like weak, and strong coupling algorithms are used[12]. The dynamics of uncompressed blood have been modelled without using a symmetrical fixed form of flow[13]. Therefore, the composite structure incorporated into the fluid equation can pass through the no-slip condition, and also the balance of contact forces is evaluated along with the interface location on the fluid-structure. These two combinations pose problems with geometric nonlinear problems and the location of the origin of the liquid is unknown. The problem of the interaction of media and fluid-structure is determined by time-dependent data from the input and output of dynamic pressure[14,15].

Arterial pressure is exerted on the walls of blood vessels by the contraction of the heart to push the blood into the vessels[16]. Furthermore, blood pressure is increased when circulation is disrupted due to increased resistance. It can be modulated through changes in heart activity, vasoconstriction, or vasodilation[17]. The factors that can change resistance are vessel length, vessel radius, and blood viscosity[18]. In addition, the circulatory system is also influenced by the speed of flow, the cross-sectional area of blood, pressure, and the work of the cardiovascular muscles and vessels[19]. Due to the complex blood flow, there are several incidents involving blood flow that have very small and large speeds to disrupt the activities of organs in the body. The problem of changes in blood flow and pressure occurs in the circulatory system.

This study proposes a blood flow velocity model using a partial differential equation with Navier-Stokes, as a partial differential equation and nonlinear continuity. This method was carried out to explain dynamic fluid blood flow in the heart blood circulation system to obtain velocity and its factors. This simulation uses the parameters of pressure, resistance, and radius geometry through Poisseuille's law. This law describes the conservation of mass and momentum equations which are solved numerically and analytically.

Theoretical Considerations and Methods:

Blood fluids have a very high correlation between resistance and volume. Due to the increase in hydrostatic pressure with respect to volume, blood fluids tend to have greater resistance. Moreover, from a hemodynamic perspective, changes in blood fluid volume can be considered incompressible. When $v(x,t) = (v_1, v_2, v_3)$, this represents the velocity of the vector function with respect to position $x = (x_1, x_2, x_3)$ and time t. Furthermore, the time-free incompressibility condition and simplification of the continuity equation can be expressed as[20]:

$$\frac{\partial v_1}{\partial x_1} + \frac{\partial v_2}{\partial x_2} + \frac{\partial v_3}{\partial x_3} = 0 \quad \ldots 1$$

The characteristics of the overall blood flow field can affect the hydrostatic pressure p under local conditions at all points of the incompressible fluid. Meanwhile, in contrast to compressible flow, where the condition of blood flow can be defined as a function of the local fluid density for each point. According to Newtonian fluid dynamics, the non-isotropic stress component has a large and proportional influence on the local velocity gradient. Therefore, the incompressible Newtonian fluid for the stress tensor component can be given by the following Eq. 2 [21]:

$$\sigma_{ij} = -p\delta_{ij} + \mu\left(\frac{\partial v_i}{\partial x_j} + \frac{\partial v_j}{\partial x_j}\right) \quad \ldots 2$$

where δ_{ij} represents the Kronecker delta, which is defined as 1 when $i = j$ and 0 when $i \neq j$.

The blood fluid flow equation is the approach used to solve the phenomenon of motion, where Eq. 2 is combined with the following equation of motion[21]:

$$\sum_{j=1}^{3} \frac{\partial \sigma_{ij}}{\partial x_j} \quad \ldots 3$$

where $\partial\sigma_{ij}/\partial x_j$ is the partial derivative of σ_{ij} for x_j then the incompressible Navier-Stokes equation is obtained[20]:

$$\rho\left(\frac{\partial v_i}{\partial t} + \sum_{j=1}^{3} v_j \frac{\partial v_i}{\partial x_j}\right) = -\frac{\partial p}{\partial x_i} + \mu\left(\sum_{j=1}^{3} \frac{\partial^2 v_i}{\partial {x_j}^2}\right) + F_i \quad \ldots 4$$

In general, Eq. 4 is solved by the unknown variables p and v to predict the fluid motion under certain conditions. In solid boundary conditions, the no-slip condition is applied, where the velocity of the fluid adjacent to the solid surface should match that of the surface.

The approach to the phenomenon of blood fluid flow can be used with the Navier-Stokes Equation as a differential form of Newton's second law concerning the movement of a fluid. This Equation states the change in momentum of fluid particles that depends on the internal and the external pressure viscous force[22]. The general Navier-Stokes Equation of an incompressible fluid flow is described as[20]:

$$\rho\frac{\partial u}{\partial t}+\rho(u\cdot\nabla)u=\nabla\cdot[-pI+\mu(\nabla u+(\nabla u)^T)]+F \quad \ldots 5$$

when the blood flow is incompressible and laminar, the Navier-Stokes Eq. 5 is described as[20]:

$$\rho(u+(u\cdot\nabla)u)=-\nabla p+\nabla\cdot\left(\mu(\nabla u+\nabla u^T)\right)+F \quad \ldots 6$$

where $\nabla\cdot u=0$ with boundary conditions for wall (u) and (p) as follows[20]:

$$u=u_0=0 \quad \ldots 7$$

$$p=p_0[\mu(\nabla u+(\nabla u)^T)]n=0 \quad \ldots 8$$

Before performing the simulation of Eq. 6, the arterial blood flow in a two-dimensional (2D) pipe is modeled, by taking a small amount of fluid (blood) (2D plane). The parameters used to obtain a model of blood flow in blood vessels consist of an artery diameter of 2.6 mm and an artery length of 10 cm, while the properties of the blood used consist of a density of 1060 kg/m^3 and a viscosity of 4×10^{-3} Pa.s.

The modeling of blood fluid flow in the blood circulation starts from the heart into the arteries and is distributed into the fine vessels (microcirculation) and returns to the veins and reaches the heart. Meanwhile, the Navier-Stokes Equation of continuity and momentum Equations for an incompressible fluid, independent of time are as follows[23]:

$$\frac{\partial U}{\partial x}+\frac{\partial V}{\partial y}+\frac{\partial W}{\partial z}=0 \quad \ldots 9$$

$$\rho\left(\frac{\partial U}{\partial t}+U\frac{\partial U}{\partial x}+V\frac{\partial U}{\partial y}+W\frac{\partial U}{\partial z}\right)=-\frac{\partial P}{\partial x}+\rho g_x+\mu\left(\frac{\partial^2 U}{\partial x^2}+\frac{\partial^2 U}{\partial y^2}+\frac{\partial^2 U}{\partial z^2}\right) \quad \ldots 10$$

$$\rho\left(\frac{\partial V}{\partial t}+U\frac{\partial V}{\partial x}+V\frac{\partial V}{\partial y}+W\frac{\partial V}{\partial z}\right)=-\frac{\partial P}{\partial y}+\rho g_y+\mu\left(\frac{\partial^2 V}{\partial x^2}+\frac{\partial^2 V}{\partial y^2}+\frac{\partial^2 V}{\partial z^2}\right) \quad \ldots 11$$

$$\rho\left(\frac{\partial W}{\partial t}+U\frac{\partial W}{\partial x}+V\frac{\partial W}{\partial y}+W\frac{\partial W}{\partial z}\right)=-\frac{\partial P}{\partial z}+\rho g_z+\mu\left(\frac{\partial^2 W}{\partial x^2}+\frac{\partial^2 W}{\partial y^2}+\frac{\partial^2 W}{\partial z^2}\right) \quad \ldots 12$$

where U, V, and W are the velocity of the blood fluid in the direction x, y, and z-axis. P is pressure, ρ is the density of the fluid and μ is viscosity.

The blood flow model is simplified in the form of a 2-dimensional flow consisting of the heart, arteries, microvessels, and veins. In the finite element of this model, a network of elements is built as shown in Fig. 1. The variation of arteries is from inlet to outlet with triangular mesh elements.

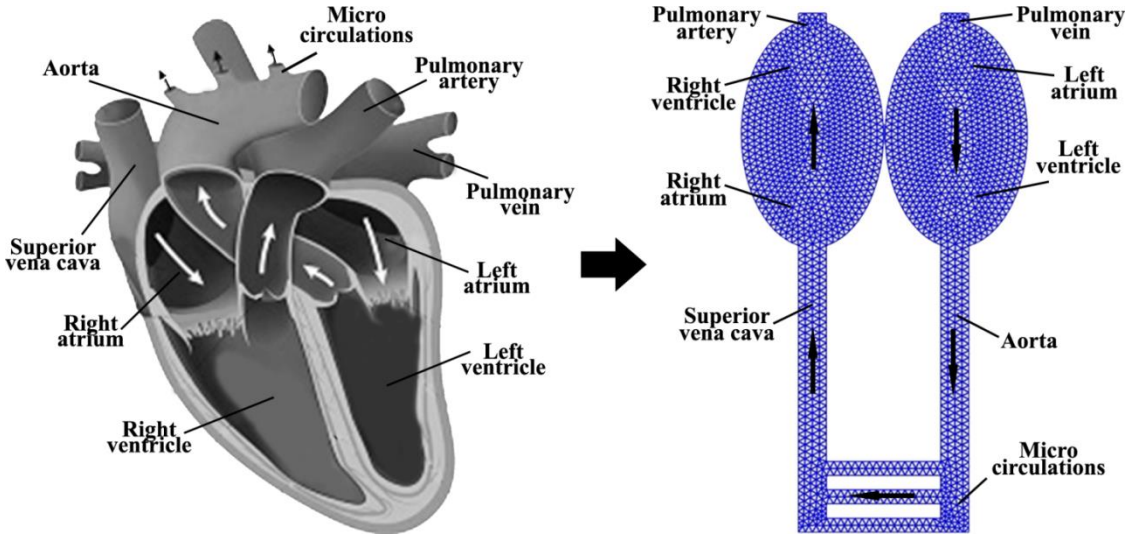

Figure 1. The blood flow media model is a triangular element tissue.

Generally, the flow of mechanical waves driven by the heart is quite complicated when the blood flow moves through the vessels. This can be simplified and described in a uniform cylindrical tube flow by prioritizing the pressure gradient, and the angular frequency ω. To solve exponential and complex wave functions, the following mathematical Equation is used[24]:

$$e^{i\omega t} = cos(\omega t) + i\, sin(\omega t) \quad \ldots 13$$

with a given pressure gradient can be expressed[25]:

$$\frac{dp}{dx} = -p' \cos(\omega t) = Re\left[p' e^{i\omega t}\right] \quad \ldots 14$$

where Re is a complex number.

Eq. 4 is solved by Bessel function and blood flow velocity is given by[26]:

$$v(r,t) = Re\left[v' e^{i\omega t}\right] \quad \ldots 15$$

$$v' = \frac{p\prime a^2}{i\mu\alpha^2}\left[1 - \frac{J_o(\alpha i^{3/2} r/a)}{J_o(\alpha i^{3/2})}\right] \quad \ldots 16$$

Equation 16 is calculated on the variation of radius, pressure, and flow velocity. The flow velocity has a pressure function that varies with the position and the moving medium. However, the equation is limited to rigid and inelastic vessels, blood types that are isotropic and homogeneous to prevent the appearance of imaginary factors in the solution.

Results and Discussion:

The blood flow model simulation is shown in Fig. 2 and explains the pattern and pressure contour. This simulation uses the velocity relative to that of the blood leaving the heart, and the speed of blood flow through the arteries increases to 1.22 cm/s from the speed of blood leaving the heart. When blood is distributed through the fine vessels (microcirculation) the velocity decreases to 0.5 cm/s. Furthermore, the decrease in velocity will be even greater when it involves more fine vessels. This is because the pressure decreases with increasing the number of channels followed by the distance of the vessels from the source of the blood returning through the veins[27].

In the human body, the viscosity of blood fluids can vary due to food and the number of fluids or drinks consumed[28]. The measure can be seen from the value of the coefficient, which increases with increasing viscosity. Therefore, it is necessary to perform simulations by varying the viscosity coefficient as shown in Fig. 3.

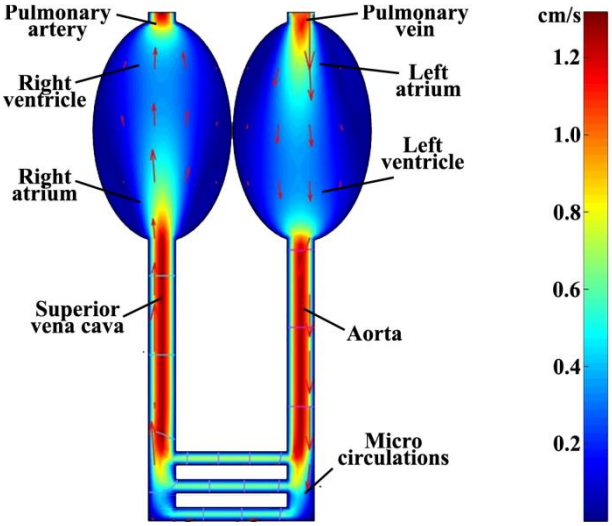

Figure 2. Blood flow of heart simulation.

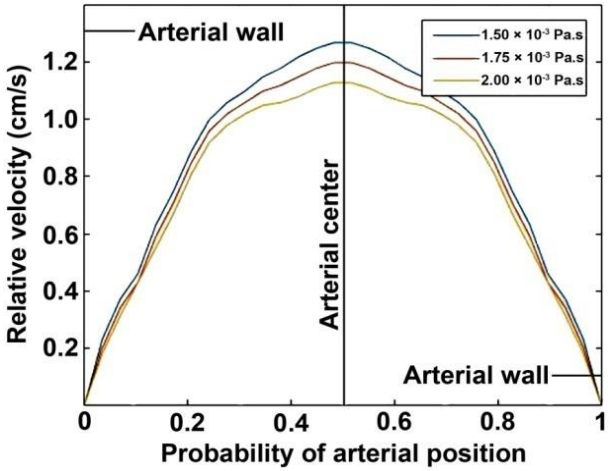

Figure 3. Blood flow velocity as a function of position.

The variation of the coefficient of blood viscosity is 1.5×10^{-3} Pa.s, 1.75×10^{-3} Pa.s, and 2×10^{-3} Pa.s and was simulated by this model. The graph in Fig. 3 shows the velocity of blood flow in a cross-section of the arteries. Furthermore, the flow velocity is zero in the walls of arteries, due to the viscosity of blood, and it is maximum in the middle[29]. The flow velocity is maximum in the middle of the arterial wall, and it is reduced in thicker blood fluid. For viscosity 1.5×10^{-3} Pa.s, the maximum blood velocity is 1.22 cm/s from the velocity of blood out of the heart. For the viscosity of 1.75×10^{-3} Pa.s and 2×10^{-3} Pa.s, the maximum velocity is 1.15 cm/s and 1.08 cm/s respectively from the velocity of blood out of the heart. The highest laminar velocity at the center of the cylindrical vessels is 0.5 and it is smaller at the edge. Furthermore, the ratio of this velocity is quite low relative to the pressure of the heart which pumps the blood throughout the body. Numerically, this has been proven through calculations with the velocity function approach to pressure using the

Bessel function as in Eq. 16. However, experimental comparisons were still conducted to obtain comparisons and validity of numerical experiments and analytical calculations.

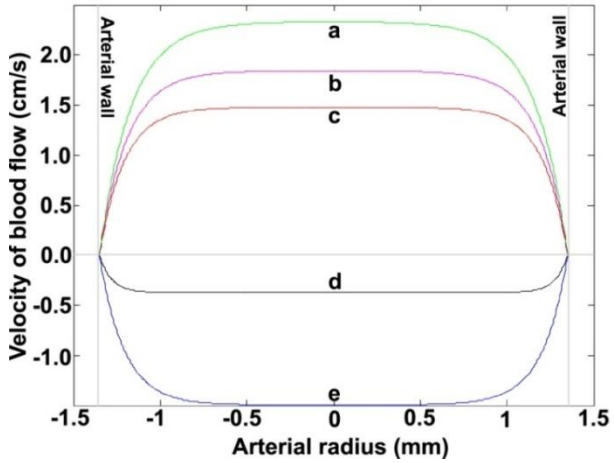

Figure 4. The movement of blood flow velocity in vessels with the same pressure gradient conditions and variations in the value of α: (a) 19.1, (b) 19.6, (c) 20.1, (d) 22.1, and (e) 23.1.

Fig. 4 shows the solution of Eq. 16 with the blood flow velocity at some point in the position of the vessel's width, with half cycles of oscillation for some of the angular frequency of the fundamental component (α) values. The graph line (c) shows aortic vessels with a diameter of 2.7 cm, heart rate of 60 bpm, blood viscosity of 3 cP, and blood densityof 1.06 g/cm^3, where $a(2\pi n/\mu)^{1/2}$. This analytical calculation is slightly higher than the numerical one on the same parameters. Meanwhile, the angular frequency of the fundamental component is[30]:

$$\alpha = 1.35\left(2\pi\frac{1.06}{0.03}\right)^{\frac{1}{2}} = 20.1 \qquad \ldots 17$$

when α = 20.1, the description of blood flow velocity does not approach a parabolic function and other variations of α with time have a pressure gradient that is not in phase. Therefore, quasi-steady is almost found, which means that the incompressible fluid provides steady flow which is approximately equal in value to the constant pressure gradient at maximum state[31]. In addition, the shear wall pressure is proportional to the slope of the blood flow velocity near the wall and tothe variation of the phase of the pressure gradient. This allows more fluid flux to flow along with the point towards the vessel's wall.

As the α decreases in the graph lines (a) and (b), the velocity performance changes in the tube and the flow velocity varies greatly in amplitude and phase near the wall. Faster flow towards the center of the cylinder. This speed is higher because the value of blood viscosity increases. Furthermore, the velocity variation in the central region and the shear stress is increasingly dependent on the pressure gradient. When the value of α is large, the interior velocity of the blood flow exceeds the fluid pressure gradient by an angle $\pi/2$. On the other hand, the shear wall pressure exceeds the fluid pressure gradient by $\pi/4$. Therefore, the interior velocity of blood flow and the shear wall pressure isin the same phase at a small pressure gradient. Negative velocity values in line graphs (d) and (e) indicate that the pressure gradient is being pulled or sucked back by the heart, and is not the same as when velocity is positive. This indicates that the pumping of blood by the heart is greater than the suction or withdrawal.

The pressure exerted by the heart on the aorta is more or less periodic, but the complexity with time variations of the pressure is much more dominant than the simple sinusoidal function. Therefore, based on Fourier analysis, the mean of the fixed components can represent pressure waves, fundamental frequencies for sinusoidal waves, and higher frequencies for harmonic waves[32]. Thus incompressible blood flow in a uniform or similar tube can be estimated by placing it on a Poiseuille flow gradient image for fixed components by isolated component analysis.

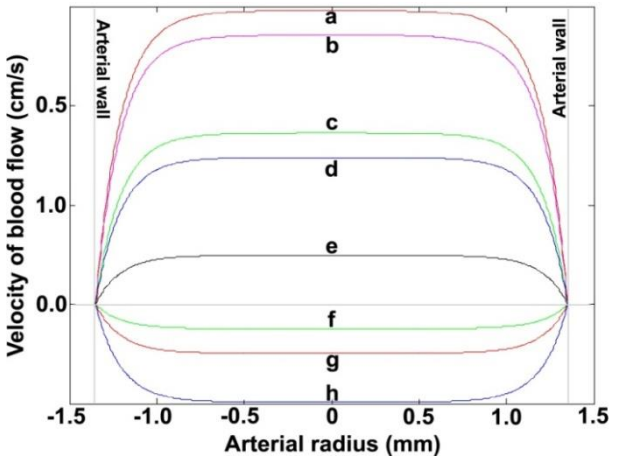

Figure 5.The movement of the velocity of blood flow in the vessels with a value of α = 20.1 constant and pressure variations: (a) 120/80 mmHg, (b) 110/70 mmHg, (c) 100/70 mmHg, (d) 100/60 mmHg, (e) 90/60 mmHg, (f) 85/60 mmHg, (g) 80/60 mmHg, and (h) 80/50 mmHg.

The predominance of inertial effects and pressure gradients tend to drive blood flow velocity. Also, the velocity description is almost similar to the tube diameter, with a narrow layer on the wall. Higher harmonic components of similar waveforms

with higher results will show the same treatment[33]. The two spatial and temporal flow variations are very different for predicting Poiseuille flow and also differ from descriptions of the same velocity, without any radial velocity variation.

When the pressure gradient decreases, the flow velocity is proportional and can either be positive or negative. The negative gradient condition indicates the flow velocity is lower than the positive at the same pressure value. This can be seen in Fig. 5.

When the α value is doubled (α = 40), the viscosity becomes denser and the pressure of blood flow near the tube wall becomes similar but remains 0 at the wall. Therefore, high viscosity results in a pressure gradient that is almost similar in the middle towards the edge of the tube as depicted in Fig. 6.

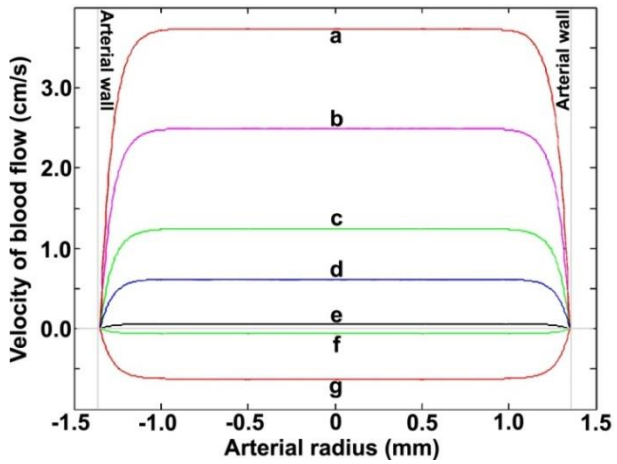

Figure 6.The movement of blood velocity in the vessels with a constant α = 40 value and pressure variations: (a) 120/80 mmHg, (b) 110/70 mmHg, (c) 100/70 mmHg, (d) 100/60 mmHg, (e) 90/60 mmHg, (f) 85/60 mmHg, and (g) 80/60 mmHg.

The trend of the flow will be quasi-steady and even reach an α value of less than 5 when the arteries are considered small with α = 5. The flow close to the heart increases the vessel's velocity and decreases the viscosity. Likewise, there is a reduced negative velocity gradient in the modulus than the positive[34]. The effect of pulse wave flow on velocity images in arteries varies widely in the arterial system according to vessel's diameter.

Conclusion:

The results of the numerical analysis show that high blood pressure from the heart circulates blood throughout the heart's blood vessels. The greater the pressure applied, the higher the speed of blood flow. However, the return blood pressure is lower at the same parameters in the cardiac vasculature due to the greater pulling effect than pushing by the pumping of the heart. The high flow velocity of 1.22 cm/s occurs in the center of the vessel which tends to be laminar and is influenced by a low viscosity factor of 1.5 × 10^{-3} Pa.s. Furthermore, the flow will approach the same extreme magnitude towards the vessel wall with almost the same velocity and radius gradient when the viscosity is high.

Acknowledgment:

The authors are grateful to The Ministry of Education, Research and Technology, Indonesia, for the research Grant's generous support in 2022. Furthermore, the authors are grateful to the Department of Physics, Mathematics and Natural Sciences Faculty, Universitas Riau, Pekanbaru Indonesia for providing research facilities and the Faculty of Applied Sciences, UniversitiTeknologi MARA, Johor, and the University of Riau for collaborative research with a simulation method.

Authors' declaration:

- Conflicts of Interest: None.
- We hereby confirm that all the Figures and Tables in the manuscript are mine ours. Besides, the Figures and images, which are not mine ours, have been given the permission for re-publication attached with the manuscript.
- The author has signed an animal welfare statement.
- Authors sign on ethical consideration's approval.
- Ethical Clearance: This project was approved by the ethics committee of the Institute for Research and Community Service, Universitas Riau based on number 451/UN.19.5.1.3/PT.01.03/2021 which is funded by the Directorate of Research and Community Service, Indonesia.

Authors' Contributions Statement:

D., T.S., and R.F.S., looking for a solution to the Navier-Stokes partial differential equation for incompressible blood flow. A.T., Y.S., and D.I., modeled the heart vessels using finite element analysis and simulated them. B.M., O., S., and H.H., analyzed numerical data from modeling using a theoretical approach to physics.

References:

1. Bao G, Bazilevs Y, Chung JH, Decuzzi P, Espinosa HD, Ferrari M, et al. USNCTAM perspectives on mechanics in medicine. J R Soc Interface. 2014 Aug;11(97):1-26.https://doi.org/10.1098/rsif.2014.0301
2. Yuan HZ, Niu XD, Shu S, Li M, Yamaguchi H. A momentum exchange-based immersed boundary-lattice Boltzmann method for simulating a flexible

filament in an incompressible flow. ComputMathAppl. 2014 Mar;67(5):1039-56.https://doi.org/10.1016/j.camwa.2014.01.006
3. Saktioto T, Fadilla FD, Soerbakti Y, Irawan D, Okfalisa. Application of fiber Bragg grating sensor system for simulation detection of the heart rate. J PhysConf Ser. 2021 Oct;2049(1):1-8.https://doi.org/10.1088/1742-6596/2049/1/012002
4. Gray RA, Pathmanathan P. Patient-specific cardiovascular computational modeling: Diversity of personalization and challenges. J CardiovascTransl Res. 2018 Apr;11(2):80-8.https://doi.org/10.1007/s12265-018-9792-2
5. Lin Q, Li T, Shakeel PM, Samuel RDJ. Advanced artificial intelligence in heart rate and blood pressure monitoring for stress management. J Ambient IntellHumanizComput. 2021 Mar;12(3):3329-40.https://doi.org/10.1007/s12652-020-02650-3
6. Jamshidi M, Ghazanfarian J. Blood flow effects in thermal treatment of three-dimensional non-Fourier multilayered skin structure. Heat Transfer Eng. 2021 Jun;42(11):929-46.https://doi.org/10.1080/01457632.2020.1756071
7. Arzani A, Gambaruto AM, Chen G, Shadden SC. Lagrangian wall shear stress structures and near-wall transport in high-Schmidt-number aneurysmal flows. J Fluid Mech. 2016 Mar;790:158-72.https://doi.org/10.1017/jfm.2016.6
8. Detmer FJ, Lückehe D, Mut F, Slawski M, Hirsch S, Bijlenga P, et al. Comparison of statistical learning approaches for cerebral aneurysm rupture assessment. Int J Comput Assist Radiol Surg. 2020 Jan;15(1):141-50.https://doi.org/10.1007/s11548-019-02065-2
9. Hassan EA, Al-Zuhairi WS, Ahmed MA. Serum cortisol and BMI in chronic diseases and increased early cardiovascular diseases. Baghdad Sci J. 2016 Jun;13(2.2NC):399-406.https://doi.org/10.21123/bsj.2016.13.2.2NCC.0399
10. Saifullah PH, Nida SM, Raoof IB. Levels of glucose-6-phosphate dehydrogenase in type 1 diabetes mellitus patients with nephropathy and cardiovascular disease complication. Baghdad Sci J. 2014 Jun;11(2):461-8.https://doi.org/10.21123/bsj.2014.11.2.461-468
11. Saktioto T, Ramadhan K, Soerbakti Y, Syahputra RF, Irawan D, Okfalisa. Apodization sensor performance for TOPAS fiber Bragg grating. Telkomnika. 2021 Dec;19(6):1982-91.https://doi.org/10.12928/telkomnika.v19i6.21669
12. Chitturi KS, Murty PSR, Babu KS. Convective flow and temperature distribution in rotating inclined composite porous and fluid layers. Songklanakarin J Sci Technol. 2022 Mar;44(2):370-80.https://doi.org/10.14456/sjst-psu.2022.52
13. Blanco PJ, Bulant CA, Müller LO, Talou GM, Bezerra CG, Lemos PA, et al. Comparison of 1D and 3D models for the estimation of fractional flow reserve. Sci Rep. 2018 Nov;8(1):1-12.https://doi.org/10.1038/s41598-018-35344-0
14. Čanić S, Galić M, Muha B. Analysis of a 3D nonlinear, moving boundary problem describing fluid-mesh-shell interaction. Trans Am Math Soc. 2020 Sep;373(9):6621-81.https://doi.org/10.1090/tran/8125
15. Defrianto D, Saktioto T, Hikma N, Soerbakti Y, Irawan D, Okfalisa O, et al. External perspective of lung airflow model through diaphragm breathing sensor using fiber optic elastic belt. Indian J Pure Appl Phys. 2022 Jul; 60(7): 561-6.https://doi.org/10.56042/ijpap.v60i7.62342
16. Bukač M, Yotov I, Zunino P. An operator splitting approach for the interaction between a fluid and a multilayered poroelastic structure. Numer Methods Partial Differ Equ. 2015 Jul;31(4):1054-100.https://doi.org/10.1002/num.21936
17. Greenstein AS, Kadir SZAS, Csato V, Sugden SA, Baylie RA, Eisner DA, et al. Disruption of pressure-induced Ca^{2+} spark vasoregulation of resistance arteries, rather than endothelial dysfunction, underlies obesity-related hypertension. Hypertension. 2020 Feb;75(2):539-48.https://doi.org/10.1161/HYPERTENSIONAHA.119.13540
18. Mirramezani M, Shadden SC. A distributed lumped parameter model of blood flow. Ann Biomed Eng. 2020 Dec;48(12):2870-86.https://doi.org/10.1007/s10439-020-02545-6
19. Magder S. The meaning of blood pressure. Crit Care. 2018 Dec;22(1):1-10.https://doi.org/10.1186/s13054-018-2171-1
20. Ershkov SV, Shamin RV, Giniyatullin AR. On a new type of non-stationary helical flows for incompressible 3D Navier-Stokes equations. J King Saud Univ Sci. 2020 Jan;32(1):459-67.https://doi.org/10.1016/j.jksus.2018.07.006
21. Ammar A, Abisset-Chavanne E, Chinesta F, Keunings R. Flow modelling of quasi-Newtonian fluids in two-scale fibrous fabrics. Int J Mater Form. 2017 Aug;10(4):547-56.https://doi.org/10.1007/s12289-016-1300-0
22. Gowthami K, Prasad PH, Mallikarjuna B, Makinde OD. Hydrodynamic flow between rotating stretchable disks in an orthotropic porous medium. Songklanakarin J Sci Technol. 2020 Mar;42:391-7.https://doi.org/10.14456/sjst-psu.2020.51
23. Ershkov SV. On Existence of general solution of the Navier-Stokes equations for 3D non-stationary incompressible flow. Int J Fluid Mech Res. 2015;42(3):206-13.https://doi.org/10.1615/InterJFluidMechRes.v42.i3.20
24. Guo X, Lu Y. Convergence and efficiency of different methods to compute the diffraction integral for gravitational lensing of gravitational waves. Phys Rev D. 2020 Dec;102(12):124076.https://doi.org/10.1103/PhysRevD.102.124076
25. Haq RU, Shahzad F, Al-Mdallal QM. MHD pulsatile flow of engine oil based carbon nanotubes between two concentric cylinders. Results Phys. 2017

Jan;7:57-68.https://doi.org/10.1016/j.rinp.2016.11.057
26. Riemer K, Rowland EM, Broughton-Venner J, Leow CH, Tang M, Weinberg PD. Contrast agent-free assessment of blood flow and wall shear stress in the rabbit aorta using ultrasound image velocimetry. Ultrasound Med Biol. 2022 Mar;48(3):437-49.https://doi.org/10.1016/j.ultrasmedbio.2021.10.010
27. Goodwill AG, Dick GM, Kiel AM, Tune JD. Regulation of coronary blood flow. Compr Physiol. 2017 Mar;7(2):321-82.https://doi.org/10.1002/cphy.c160016
28. Sempionatto JR, Lin M, Yin L, Pei K, Sonsa-ard T, de Loyola Silva AN, et al. An epidermal patch for the simultaneous monitoring of haemodynamic and metabolic biomarkers. Nat Biomed Eng. 2021 Jul;5(7):737-48.https://doi.org/10.1038/s41551-021-00685-1
29. Toghraie D, Esfahani NN, Zarringhalam M, Shirani N, Rostami S. Blood flow analysis inside different arteries using non-Newtonian Sisko model for application in biomedical engineering. Comput. Methods Programs Biomed. 2020 Jul;190:1-8.https://doi.org/10.1016/j.cmpb.2020.105338
30. Rukshin I, Mohrenweiser J, Yue P, Afkhami S. Modeling superparamagnetic particles in blood flow for applications in magnetic drug targeting. Fluids. 2017 Jun;2(2):29.https://doi.org/10.3390/fluids2020029
31. Liu K, Yin D, Su H. Transient transfer shape factor for fractured tight reservoirs: Effect of the dynamic threshold pressure gradient in unsteady flow. Energy Sci Eng. 2020 Jul;8(7):2566-86.https://doi.org/10.1002/ese3.686
32. Dellavale D, Rosselló JM. Cross-frequency couplings in non-sinusoidal dynamics of interacting oscillators: Acoustic estimation of the radial position and spatial stability of nonlinear oscillating bubbles. UltrasonSonochem. 2019 Mar;51:424-38.https://doi.org/10.1016/j.ultsonch.2018.07.026
33. Wang H, Krüger T, Varnik F. Geometry and flow properties affect the phase shift between pressure and shear stress waves in blood vessels. Fluids. 2021 Nov;6(11):1-16.https://doi.org/10.3390/fluids6110378
34. Karvelas E, Sofiadis G, Papathanasiou T, Sarris I. Effect of micropolar fluid properties on the blood flow in a human carotid model. Fluids. 2020 Sep;5(3):1-16.https://doi.org/10.3390/fluids5030125

التحقيق العددي للمعلمات الفيزيائية في الأوعية القلبية كعلم دعم طبي جديد لخصائص تدفق الدم المعقدة

أنديكا ذويبة[1] ديفريانتو[1] توتو ساكتيوتو*[1] يان سورباكتي[1]
زهرة ميزيا[1] رومي فضلي سياحبوترا[2] أوكفاليسا[3]
شمسودهها[4] ديدي إيراوان[5] هاريانا هيري[6]

[1] قسم الفيزياء ، كلية الرياضيات والعلوم الطبيعية ، جامعة رياو ، بيكانبارو ، إندونيسيا.
[2] قسم الفيزياء ، كلية الرياضيات والعلوم الطبيعية والصحة ، جامعة المحمدية رياو ، بيكانبارو ، إندونيسيا.
[3]قسم هندسة المعلوماتية ، كلية العلوم والتكنولوجيا ، جامعة الإسلام نيجري سلطان سياريف قاسم ، بيكانبارو ، إندونيسيا.
[4] قسم الرياضيات ، كلية الرياضيات والعلوم الطبيعية ، جامعة رياو ، بيكانبارو ، إندونيسيا.
[5] قسم التربية الفيزيائية ، كلية تدريب المعلمين والتعليم ، جامعة رياو ، بيكانبارو ، إندونيسيا.
[6] قسم الفيزياء ، كلية العلوم التطبيقية ، جامعة التكنولوجيا مارا ، شاه علم ، ماليزيا

الخلاصة:
تقترح هذه الدراسة نهجًا رياضيًا وتجربة عددية لحل بسيط لتدفق الدم القلبي إلى الأوعية الدموية للقلب. تمت دراسة نموذج رياضي لتدفق الدم البشري عبر الفروع الشريانية وحسابه باستخدام معادلة نافييه-ستوكس التفاضلية الجزئية مع تحليل العناصر المحدودة (FEA). علاوة على ذلك ، يتم تطبيق FEA على التدفق الثابت للسوائل اللزجة ثنائية الأبعاد من خلال أشكال هندسية مختلفة. تتحدد صلاحية الطريقة الحسابية بمقارنة التجارب العددية مع نتائج تحليل الوظائف المختلفة. أظهر التحليل العددي أن أعلى سرعة لتدفق الدم تبلغ 1.22 سم / ثانية حدثت في مركز الوعاء الذي يميل إلى أن يكون رقائقيًا ويتأثر بعامل لزوجة منخفض قدره 0.0015 باسكال. بالإضافة إلى ذلك ، تحدث الدورة الدموية في جميع الأوعية الدموية بسبب ارتفاع الضغط في القلب ويقل الضغط عندما يعود من الأوعية الدموية بنفس المعايير. أخيرًا ، عندما تكون اللزوجة عالية ، تميل المقادير القصوى لتدفق الدم نحو جدار الوعاء الدموي بنفس سرعة التدرج ونصف قطره تقريبًا.

الكلمات المفتاحية: تدفق الدم، قلب، أوعية،نافيير-ستوكس،تحليل العناصر المحدودة.